**Atmospheric
Chemistry
and Physics
Discussions**

ACPD

4, 6149–6183, 2004

NO$_y$ instrument
aboard MOZAIC
in-service aircraft

A. Volz-Thomas et al.

Title Page

Abstract	Introduction
Conclusions	References
Tables	Figures

|◄ | ►|

◄ | ►

Back | Close

Full Screen / Esc

Print Version

Interactive Discussion

© EGU 2004

Measurements of total odd nitrogen (NO$_y$) aboard MOZAIC in-service aircraft: instrument design, operation and performance

A. Volz-Thomas, M. Berg, T. Heil, N. Houben, A. Lerner, W. Petrick, D. Raak, and H.-W. Pätz

Institut für Chemie und Dynamik der Geosphäre II: Troposphäre, Forschungszentrum Jülich, Jülich, Germany

Correspondence to: A. Volz-Thomas (a.volz-thomas@fz-juelich.de)

Abstract

A small system for the unattended measurement of total odd nitrogen (NO$_y$, i.e., the sum of NO and its atmospheric oxidation products) aboard civil in-service aircraft in the framework of MOZAIC is described. The instrument employs the detection of NO by its chemiluminescence with O$_3$ in combination with catalytic conversion of the other NO$_y$ compounds to NO at 300°C on a gold surface in the presence of H$_2$. The instrument has a sensitivity of 0.4–0.7 cps/ppt and is designed for unattended operation during 1–2 service cycles of the aircraft (400–800 flight hours). The total weight is 50 kg, including calibration system, compressed gases, mounting, and safety measures. The layout and inlet configuration are governed by requirements due to the certification for passenger aircraft. Laboratory tests are described regarding the conversion efficiency for NO$_2$ and HNO$_3$ (both >98%). Interference by HCN and NH$_3$ is 100% and <1%, respectively. The time response (90% time) of the instrument is <1 s for NO$_2$ and 150 s for HNO$_3$, the latter being caused by memory effects in the 80 cm long inlet line.

1. Introduction

Nitrogen oxides play a key role in atmospheric photochemistry by catalysing the recycling of free radicals and the formation of ozone (Chameides and Walker, 1973; Crutzen, 1973; Liu et al., 1980). Despite of the many field measurements including campaigns with research aircraft (c.f., Emmons et al., 1997, 2000), the distribution and variability of nitrogen oxides is still not well known, in particularly in the upper troposphere and lower stratosphere (UT/LS). The existing data suggest a large variability and significant differences in the partitioning of NO$_y$ into active compounds, i.e., NO$_x$ (NO + NO$_2$) and reservoir species such as HNO$_3$, HNO$_4$, PAN and other organic nitrates. The pathways for recycling of NO$_x$ from, e.g. HNO$_3$, are not well understood. The different sources of NO$_y$ to the upper troposphere include lightning and emissions by aircraft (in the form of NO$_x$), uplifting of surface emissions (variable NO$_x$/NO$_y$

**NO$_y$ instrument
aboard MOZAIC
in-service aircraft**

A. Volz-Thomas et al.

ratio) and downward transport from the stratosphere (mainly HNO$_3$, c.f., Neuman et al., 2001).

Regular surveys of the NO$_y$ distribution in the UT/LS can help to gain a better understanding of the downward transport of O$_3$ from the stratosphere (c.f., Murphy et al., 1993; Murphy and Fahey, 1994) and to discriminate the impact of aircraft emissions on the UT/LS from the influence of convective transport of surface emissions.

While it has become possible to derive important information on the tropospheric column of NO$_2$ from space-borne remote sensing (Richter and Burrows, 2002), it is not yet possible to obtain remote sensing data with the spacial resolution required to study the tropopause region. The only climatological dataset of NO$_x$ in the UT/LS comes from the NOXAR project (Measurements of Nitrogen Oxides and Ozone Along Air Routes, (Brunner et al., 2001).

We describe here a small NO$_y$ instrument that was built in the framework of the European Project MOZAIC (Measurements of Ozone and Water Vapour aboard Airbus In-service Aircraft, (Marenco et al., 1998) and has been certified for unattended operation aboard passenger aircraft. The instrument was installed aboard an A-340-300 long-haul aircraft of Deutsche Lufthansa AG and is in operation since January 2001.

2. The NO$_y$ instrument

The design of the NO$_y$-instrument for MOZAIC followed largely that of previous airborne instruments, e.g., (Drummond et al., 1985; Ridley and Grahek, 1990), by combining a chemiluminescence detector (CLD) for NO with a catalytic converter for conversion of the different NO$_y$ compounds to NO (Fahey et al., 1985; Gerbig et al., 1996; Kliner et al., 1997). An overview of the main components is given in Fig. 1. Major constraints were weight, size, and the supply of compressed gases. The latter precluded the use of large sample flow rates as required for achieving maximum sensitivity. Other constraints were posed by the certification for passenger aircraft and by the requirement for unattended deployment during at least one full service cycle of the aircraft (>50 flights

or >400 flight hours), including measures against contamination during landing or take off and while the aircraft is at ground with or without electrical power. The individual components of the instrument are described in the following.

2.1. The CLD

The detection of NO is based upon the well known chemiluminescent reaction with ozone (Clough and Thrush, 1967).

$$NO + O_3 \rightarrow NO_2 + O_2 \qquad (1a)$$

$$NO + O_3 \rightarrow NO_2^* + O_2 \qquad (1b)$$

$$NO_2^* \rightarrow NO_2 + h\nu \ \ (\lambda > \ 600 \ nm) \,. \qquad (2)$$

For this purpose the sample air is mixed, inside a reaction chamber fitted with a red-sensitive photomultiplier tube (PMT), with a small flow (here 10 ml/min STP) of O_2 containing O_3. Interference from chemiluminescence occurring at shorter wave lengths due to, e.g., SO_2 or HCHO is blocked by a red filter in front of the PMT. Interferences by the reactions of O_3 with olefinic hydrocarbons, which create emission in the near infra red, is corrected by employing a so-called chemical zero mode, where the O_3 air mixture is passed through a relaxation volume before entering the reaction chamber (Drummond et al., 1985). The relaxation volume is chosen such that the residence time of the mixture is large enough that NO is oxidised to about 90% whereas the concentration of olefins, which react with O_3 at least 2 orders of magnitude much more slowly than NO, are changed only by a few percent. The NO mixing ratio in the sampled air is then derived from the difference between the measure and zero modes.

2.1.1. Reaction chamber

The design of the reaction chamber (see Fig. 2) was adapted from (Ridley and Grahek, 1990), using a gold plated cylindrical stainless steel cell (30 cm^3 volume) connected

NO$_y$ instrument aboard MOZAIC in-service aircraft

A. Volz-Thomas et al.

NO$_y$ instrument aboard MOZAIC in-service aircraft

A. Volz-Thomas et al.

to a photomultiplier (PMT). The reaction cell is separated from the PMT housing by means of two 1mm thick windows (Schott WG320, and RG610), which provide thermal insulation and discriminate light from wavelengths below 600 nm. The space between the cell window and the red filter, as well as the PMT housing, are purged with a small flow of O$_2$ (0.2 ml/min). The temperature of the cell is controlled at 20°C.

The photomultiplier (Thorn-EMI 9828A, 1″diameter S20 photocathode, selected for enhanced red sensitivity and low dark current) is operated in the photon counting mode. The preamplifier (Thorn-EMI C637AFP) is located inside the housing and feeds into a fast discriminator (10 ns peak resolution) which delivers TTL pulses to the counter board in the PC-104 computer system (see below). The PMT is cooled to −12°C by four Peltier elements (Melcor, CPO.8-71-06L-2-RTV) mounted at the front part of the housing. A copper mesh between the photocathode and the red filter enhances the heat transfer. The Peltier elements are air cooled via heat sinks and two small fans.

Sample air and O$_3$ enter the cell through concentric slits around the cell window and are exhausted through a 4 mm diameter hole in the back flange. For switching between measure and zero modes, both sample air and O$_3$ flow paths are altered by means of two magnetic 3/2-way valves (Entegris PFA 203-3414-215 for sample air, Fluid Automation SS 6-311N102-41EDCEDE, for O$_3$). The zero mode is activated every 28 s for 4 s. The relaxation volume is made of a 35 cm long, 6mm ID FEP tube. All tubes connected to the reaction chamber are covered with black heat shrink and the PFA valve is placed inside an aluminium housing in order to prevent light leaks.

2.1.2. Ozone generator

The self-built ozone generator consists of a coaxial discharge tube made of an 18 cm long, 4 mm ID ceramic tube (Alsint 99.7) with a 3 mm OD stainless steel electrode which is fed with 3.7 kV, 400 Hz from a high voltage transformer connected to the aircraft power supply. The end fittings of the discharge tube are made of FEP. The outer electrode is made from copper and is connected to the housing for cooling. A 3 MOhm resistor in the high voltage line serves to protect the transformer from tran-

sients. The oxygen flow (10 ml/min STP) is controlled by the central oxygen pressure regulator (see Fig. 1) and a quartz capillary upstream of the discharge tube. A second capillary mounted downstream of the tube serves to control the pressure in the discharge at 1.15 bar, which provides the maximum ozone yield.

2.2. Pneumatics, pump

A small two-stage, four-head membrane pump (Vacuubrand GmbH, MD 1 Vario-SP) is used in combination with a downstream-pressure regulator (Brooks TR 5866/A1-D-2-B-2-B-B-2) and a critical orifice upstream of the CLD to maintain the flow through the CLD. The pressure in front of the orifice (0.6 mm diameter) is maintained by the pressure regulator at 30 mbar for a constant sample flow of 90 ml/min STP. The pump is equipped with PTFE-coated membranes and Kalrez valves for resisting high ozone concentrations. In addition, a charcoal filter is place between reaction cell and pump for protecting the pump and for preventing hazardous ozone concentrations being exhausted from the NO_y-instrument because of safety requirements.

2.3. Catalytic converter

The catalytic converter consists of a 10 cm long 1.8 mm ID gold tube, which is mounted inside an oven which is kept at a nominal temperature of 300°C. The oven heater (Philips Thermocoax SEI10/100) is silver-soldered around a stainless steel mandrel, which provides a reasonably uniform temperature profile, as shown in Fig. 3. The heater is powered by 28 V DC via a temperature controller (Hengstler type 901) and a solid state relay. A bimetal safety switch is installed at the oven housing. The heater is somewhat oversized in order to enable heating of the converter to 450°C within 10 min after take-off for cleaning.

The converter is operated at variable pressure (250–1000 mb) and constant mass flow. The connection between inlet and gold tube is critical, both in terms of time response (90% of NOy may consist of HNO_3 in the lower stratosphere) and safe oper-

NO_y instrument aboard MOZAIC in-service aircraft

A. Volz-Thomas et al.

Title Page

Abstract | Introduction

Conclusions | References

Tables | Figures

◄ | ►

◄ | ►

Back | Close

Full Screen / Esc

Print Version

Interactive Discussion

ation. At the upstream side, a 30 mm long, SS-tube (3 mm ID, 4 mm OD) is soldered onto the gold tube. The SS tube is inserted into the inlet manifold, where it is sealed with a 4mm PFA-Ferrule and Valco nut. A 20 mm long, 3 mm OD borosilicate tube (Fig. 4) is inserted into the SS tube so that the sample air has no contact with the SS surface. The construction serves to keep the temperature of the FEP manifold (see below) at 50°C when the converter temperature is set at nominally 300°C and when the tip of the gold tube is at 250°C (see Fig. 3). In earlier tests, it had been noted, that overheating the FEP or PFA tubes produced large background signals. At the downstream side, a SS-reducer to 1/8″ is soldered over the gold tube.

The length of the gold tube is sufficient for mass flow rates of up to 300 scc/min (c.f., Murphy and Fahey, 1987), as experimentally verified by shortening a tube by a factor of three. The longer tubes are used because of the long operating cycles of the MOZAIC instrument, without the possibility for cleaning in between flights.

H_2 is used as a reducing agent instead of CO (c.f., Kliner et al., 1997), because of unsolvable problems with the certification of CO for operation on passenger aircraft due to its toxicity in addition to flammability. Whilst certification problems had first been encountered for H_2 as well, this was finally solved by using a metal hydride storage device. The H_2 storage container (Hycob GmbH, HS20) consists of a SS cylinder (Hoke, type 4HS75, 75 ml volume) containing 120 g of a Ti alloy (Ti0.95Zr0.05Mn0.15V0.04Fe0.01). The thermodynamics of this alloy allow its use without a pressure regulator. The H_2 flow rate is controlled by the equilibrium pressure of H_2 over the alloy and a capillary, which is directly mounted at the cylinder valve. As shown in Fig. 5, the H_2 pressure changes only moderately with temperature. For a freshly filled cylinder containing 2g of H_2, flow rates remain between 0.2 and 0.4 ml/min over a temperature range of 10–50°C (The temperature of the avionic compartment varies only between 15 and 25°C during flight). During seven weeks of operation the flow rate decreases to 0.05 ml/min, which is still more than sufficient for maintaining the conversion efficiency of the converter for NO_2 and HNO_3 at >95%.

NO$_y$ instrument aboard MOZAIC in-service aircraft

A. Volz-Thomas et al.

Title Page

Abstract	Introduction
Conclusions	References
Tables	Figures

◀︎ ▶︎

◀ ▶

Back Close

Full Screen / Esc

Print Version

Interactive Discussion

2.4. Inlet configuration

The design of the inlet configuration was one of the most problematic parts of the whole enterprise. The limited space available on the existing MOZAIC flange together with the safety requirements for, e.g., smoke detection and overheating protection, as well

5 as the need for regular removal of the NO_y instrument for maintenance and quality control, precluded the integration of the gold converter into the inlet probe. It was therefore decided to integrate the converter into the housing of the NO_y instrument, with the disadvantage of having to use an 80 cm long inlet line.

Similarly, a decision had to be made on the configuration of the air intake. After
10 several tests, it was decided to adapt the Rosemount probe (Model 102B) deployed in MOZAIC since 1994 for temperature and humidity measurements (c.f., Gierens et al., 1999; Helten et al., 1998; Helten et al., 1999) for the NO_y inlet. The schematics of the design are shown in Fig. 6. The FEP inlet line is inserted into the (10 mm ID) side arm of the probe such that the tip is located about 2 mm behind the bend. The part
15 of the inlet tube inside the Rosemount probe is heated to 20°C by a PTFE-insulated heating wire wound tightly around the tube and fixed by two layers of ceramic tape. A 0.5 mm DIA thermocouple and a temperature controller (PMA, type KS10) serve to maintain a constant temperature. A thin wall SS-tube of 8 mm OD serves as a liner in order to prevent the inlet line from touching the walls of the Rosemount probe.

20 Inside the NO_y-instrument, the inlet line is connected to a manifold (Fig. 4) made from FEP, which contains ports for the addition of zero air, calibration gases and hydrogen, pressure measurement, and a by-pass around the gold converter that allows to make measurements of NO. The port opposite to the inlet line is connected to a backward facing 4mm ID tube on the aircraft flange that serves for purging of the inlet line and for
25 venting of the calibration gases and the pump exhaust.

At cruise altitude, the total flow rate through the inlet line is 900 ml/min STP and the pressure in the inlet manifold is 250 mbar. The resulting residence time in the inlet line is 0.05 s. When the aircraft is grounded, the connection between manifold and exhaust

line is closed by a magnetic valve and the inlet line is back-flushed with the O_2 flow from the ozone generator.

2.5. Calibration

In flight calibration of the CLD is achieved by adding a small flow of a calibration gas
5 (10 ppm NO in ultra-pure N_2) to the sample flow of the instrument. The calibration gas is contained in a 400 ml PTFE-coated SS cylinder (Whitey 304L-HDF4-400-T). The flow rate of the calibration gas (0.2 ml/min) is controlled by two SS pressure regulators and a quartz capillary. A second capillary (flow rate 2 ml/min) connected to the exhaust serves the purpose to maintain a shorter residence time of the calibration gas
10 in the pressure regulators and lines. All flow rates are determined from pressure measurements made upstream (P_1) and downstream (P_2) of the capillaries according to Hagen-Poiseuille's Law (Eq. 3).

$$dM/dt = fr_i^*(P_1^2 - P_2^2) \tag{3}$$

The flow resistances fr_i of the capillaries are determined in the laboratory with an
15 absolute flow meter (Gillian) and are checked during each maintenance cycle. The relevant pressures (see Fig. 1) are measured by small sensors (Sensortechnics, type 144SB00xA-PCB) and are recorded at a rate of 1 Hz. The sensors are calibrated during maintenance against a reference standard (Leitenberger GmbH, PC6-005-C-2). The stability of the calibration of the pressure sensors proved better than ±0.5% .
20 For in-flight calibration of the conversion efficiency, a miniature gas phase titration system (GPT) is used to convert the NO partially to NO_2 (Eq. 1). The ozone is made in a flow of 0.2 ml/min of O_2 in a 1/16″ PFA tube which is irradiated by a Hg-lamp. The O_3 concentration is adjusted to 70±10% of the NO concentration in the calibration gas by changing the irradiated length of the PFA-tube. The O_2 is always flowing and
25 the NO_2 calibration is initiated by actuation of a shutter in between the Hg-lamp and the PFA tube (see Fig. 1). The degree of titration is checked in flight by measuring the calibration gas with and without the shutter activated in both modes of the NO_y

instrument, i.e., through the converter and bypassing the converter. In addition, the O_3 concentration is measured before being mixed with the calibration gas, in a small photometer (l=40 mm; ID=0.8 mm), using the light of the same Hg-lamp as used for generating the O_3.

5   The background of the instrument is also determined in flight by overflowing the inlet manifold with O_2. The results of this procedure compare within the statistical errors with measurements of zero air. The conversion efficiency for HNO_3 is checked during maintenance in the laboratory (see below).

2.6. Safety features

10   In order to comply with the certification requirements for passenger aircraft, most components are selected for respective specifications. Furthermore, the NOy instrument is integrated into one box, which is equipped with provisions for overheating protection and an avionic smoke detection system. The latter also provides the ventilation for the entire system. The heater for the inlet line and the de-icing heater of the Rose-
15   mount probe are disabled when the aircraft is grounded by the landing gear signal of the aircraft and by pressure switches (600 mb) connected to the NOy inlet line.

2.7. Data acquisition and control

A PC-104-computer system is used for instrument control and data acquisition/storage. It contains a cpu board with intel pentium processor, a 1Gb Flash Memory Disk (SAN
20   Disk Corp.), and several I/O boards containing ten 16-bit counters, digital I/Os and 16 analog I/Os with opto-coupled inputs and individual pre-amplifiers for signal conditioning, as well as 16 relays for switching of the magnetic valves. The PC-104 system is powered via a 24 V vehicle power supply with battery back-up (NiMH). The data acquisition system is enclosed in an aluminium box for EMI protection.
25   The NO_y-instrument is powered from the aircraft 115 V/400 Hz power supply. The main power is distributed via a line filter and fuses to the ozone generator and to a

switching power supply (Vicor Flatpac, Model VI-MUL-IQ-VIC; input 115 V, 400 Hz, output 24 V DC, 400 VA), which provides the power to the data acquisition unit and from there to the other units.

The software package for instrument control, data acquisition and storage is written in Borland Delphi version 5 under Windows 98SE. Data from the photon counter are stored at a rate of 10 Hz in order to allow the detection of short spikes, as highlighted in Fig. 7. Housekeeping data (pressures, temperatures) are stored as 1 s averages. The program controls the different measurement modes of the instrument and enables the in-flight calibration cycles for NO, NO_2, and instrument background. The program is always running when the aircraft is under power. When power is disconnected, the PC-104 continues operation from the battery pack. If power is disconnected for longer than 15 s, the program and operating system are terminated. Upon power on, the whole process starts automatically. As long as the aircraft is grounded, the program keeps the instrument in stand-by mode, in which the inlet line is back-flushed with O_2 from the ozone generator. Operation is started after take-off, when the landing gear is taken in. In addition, the program monitors the pressure difference between inlet manifold and exhaust line, which is a measure of the aircraft speed.

During the first 30 min of each flight, the gold converter is heated to 450°C for cleaning. During this time, the by-pass is active so that the instrument measures NO. Thereafter, the gold converter is reset to 300°C and the regular NOy measurement cycle is started. Calibration cycles and background determination (see Fig. 8) are configured by entries in a configuration file. At the beginning of the operation in MOZAIC, 2–3 calibration cycles with NO and NOx measurements, both in the NOy and NO measuring modes, were made during each flight (every 4 h). The background was determined every 2 h for 5 min. This procedure was later relaxed to 1 calibration and 1 background determination per flight. The chemical zero mode of the CLD is actuated every 28 s for 4 s.

2.8. Maintenance and QA/QC

Extensive pre- and post-flight calibrations are made in the laboratory using a primary standard (10 ppm NO in ultra pure N_2, BOC/Messer Griesheim). The procedure includes:

5
1. A calibration with the pre-diluted primary standard provided to the inlet line at excess flow in order to determine the sensitivity of the instrument and the transmission of the converter for NO.

2. A calibration with the primary NO-standard connected to the internal calibration system of the instrument (in both modes) in order to obtain information on possible losses of NO in the calibration system or possible changes in the capillaries/pressure sensors used for determination of the flows. The conversion efficiency is determined in the same experiment with the internal GPT system.

3. An internal calibration with the internal NO cylinder in order to observe possible changes in the NO mixing ratio of the in-flight standard during the previous operating cycle and for calibrating the internal NO-cylinder after refilling for the next cycle.

4. The conversion efficiency for HNO_3 is determined with the permeation source described below.

Other maintenance includes:

20
Every cycle, the hydride cylinder is replaced (and refilled at factory), the internal NO cylinder is refilled, the charcoal in the ozone scrubber is replaced. Safety inspections include a complete leak test, electrical and mechanical inspection, in particular of safety relevant components (e.g., pressure switches), documentation for reinstallation, and final calibration as outlined above. Cleaning/replacement of the gold tube is done if

25
necessary because of increased background or when the conversion efficiency has dropped below 95%.

Every third cycle (or earlier if necessary), the membrane pump is replaced (and serviced at the factory), the ozone generator is refurbished with a new discharge tube, the reaction chamber of the CLD is cleaned, and the pressure sensors and flow resistors are re-calibrated. The latter is always performed if discrepancies between experiments 1. and 2. are observed.

3. Laboratory tests

Laboratory tests were conducted for establishing the conversion efficiency of the converter and the time response of the inlet system for NO_2 and HNO_3, and for interference from atmospheric constituents that do not fall into the NO_y family. For this purpose, a multi source permeation system was set up, using commercial permeation tubes (Kintek). The permeation system holds four different permeation tubes (PT), which are placed inside individual stainless steel containers mounted inside a temperature controlled oven at 35°C. The tubes are fed with zero grade air at 4 atm and the air flow is controlled by capillaries downstream of the permeation tubes. The effluent is then added either into the inlet of the NO_y instrument or is pre-mixed with a known flow of zero air. For each PT, a pair of capillaries is used with a split ratio of 1:5, enabling calibrations at concentrations differing by a factor of five to be made without changing the conditions of the permeation sources or the dilution flow.

The permeation rates for HNO_3, HCN and NH_3 were determined by ion chromatography against weighted standards in samples obtained by absorption of the effluent from the PTs in aqueous solutions (pure H_2O for HNO_3, 0.1 n NaOH for HCN and 0.1 n H_2SO_4 for NH_3). The permeation rate for NO_2 was determined with the NO_y instrument by comparison against the GPT system.

3.1. Conversion efficiency and interferences

Figure 9 shows the conversion efficiency of the gold converter for NO_2 (13 ppb), HNO_3 (14 ppb) and HCN (83 ppb) as a function of converter temperature, both for H_2 (filled symbols) and CO (open symbols), at flow rates of 0.2 ml/min STP. For HNO_3 and NO_2, significant conversion is already observed at room temperature and conversion efficiencies above 90% are found at 200°C. The results for CO and H_2 as reducing agent are similar within the experimental uncertainties.

The conversion efficiency for HCN is also displayed in Fig. 9. For experiments with H_2, HCN is converted to 100% at 300°C, in agreement with the results of Kliner et al. (1997), for dry air. When H_2 is replaced by CO, however, the entire curve for HCN is shifted by about 100°C and quantitative conversion is only reached at temperatures >400°C. This results is in general agreement with those obtained by other investigators, e.g. Weinheimer et al. (1998), who found conversion efficiencies below 40% for converters operated with CO at 300°C.

Conversion of NH_3 was negligible (i.e. <1%) for either CO or H_2 at temperatures up to 400°C.

Because of the sufficient length and the relatively homogeneous temperature profile of the converter, we found no significant pressure dependence of the conversion efficiency for NO_2 and HNO_3, although the temperature of the gold tube is actually less than 300°C (Fig. 3). We should like to note that operation of the gold tube at 50°C higher temperatures, which was accidentally done during one service period, did not give different results in terms of NOy to O_3 ratios. Losses of NO were not observed with our converter in the presence of H_2, similar to the results of Kliner et al. (1997). The transmission for NO always remained at >98%, except for a situation when the converter was heavily contaminated as indicated by very low conversion efficiencies for NO_2 and HNO_3.

Title Page

Abstract | Introduction

Conclusions | References

Tables | Figures

◄◄ | ►►

◄ | ►

Back | Close

Full Screen / Esc

Print Version

Interactive Discussion

NO$_y$ instrument aboard MOZAIC in-service aircraft

A. Volz-Thomas et al.

3.2. Time response

The response time of the inlet configuration is important for, e.g., the interpretation of the correlation between ozone and NO$_y$, because of the strong layering observed from, e.g., the MOZAIC ozone data (Thouret et al., 2000) and in particular the fast transitions observed when the aircraft cross the tropopause (c.f., Thouret et al., 1998). HNO$_3$ is the most important species to be considered because of its larger affinity to surfaces as compared to NO$_x$ and because it comprises about 90% of NO$_y$ in the lower stratosphere (c.f., Neuman et al., 2001).

We investigated the behaviour of inlet lines of different lengths made of PTFE, PFA and FEP tubing at different temperatures, before the first MOZAIC III test flight in 2000. The results are shown in Fig. 10. Different from Neuman et al. (1999), we found the behaviour of FEP superior to PFA in terms of memory, which lead to the use of FEP for the inlet line and inlet manifold.

The results for the actual MOZAIC inlet (about 80 cm, 1/8″ FEP tubing, controlled at 20°C) are shown in the lower panel of Fig. 10. They were obtained with the following setup: The HNO$_3$ permeation source (1 ml/min) was connected to a 1/32″ OD PFA tube mounted inside a sliding injector made from borosilicate glass with an extruded tip. The sliding injector was mounted opposite to the inlet line inside a glass flow tube. Excess zero air (5 l/min) was introduced into the flow tube passing along the inlet line and being exhausted through a metering valve and pump connected to a port behind the injector. In this position, the HNO3 flow from the injector is vented together with the zero air and does not reach the inlet line. For injection, the sliding injector is moved forward against a stop such that the tip of the 1/32″ tube is inserted 3 mm into the inlet line. In this position, the flow from the PT enters the inlet line. The setup allows to inject into and remove HNO$_3$ from the inlet line within less than 1 s.

The pressure in the flow tube was varied between 1 atm and 300 mb, corresponding to the ambient conditions during flight. The flow rate through the inlet line was adjusted to match exactly the conditions during flight by adjusting the pressures in the inlet

manifold and in the exhaust of the NO_y instrument according to the data recorded in-flight. The negative ram pressure at the exhaust was simulated with a vacuum pump and metering valve connected to the exhaust line of the NOy instrument.

4. Discussion

4.1. Sensitivity

Assuming optimum design of the other components, i.e., reaction cell, PMT and ozone generator, the sensitivity of the CLD is proportional to the volume flow provided by the pump. The pump chosen for the MOZAIC instrument maintains a total flow rate (sample and ozone) of 100 ml/min STP at a cell pressure of <10 mbar, corresponding to a volume flow rate of about 200 ml/s through the reaction cell. It has the best efficiency in its weight class and is equipped with a lightweight brushless 28 V DC motor that has optimum performance with regard to electromagnetic interference, an important requirement for installation inside the avionic bay of the aircraft. A larger sensitivity would have been achievable only with large increases in weight, which was not possible within the framework of MOZAIC, because the airlines carrying the equipment without charging for transportation cost.

4.2. Inlet system

The Rosemount probe was chosen as inlet because a simple forward facing probe would lead to size dependent enrichment factors for atmospheric aerosol (c.f., Fahey et al., 2001), thus rendering the interpretation of the NO_y-data difficult. Backward sampling, on the other hand, while discriminating against aerosol nitrate, has the strong disadvantage of the negative ram pressure that does not allow a large sample flow through the sampling line without employing an additional pump (the sample flow through the converter and CLD is only 90 ml/min STP). The Rosemount probe combines both advantages, by acting as a virtual impactor, thereby separating the particles

Title Page

Abstract	Introduction
Conclusions	References
Tables	Figures

◄ | ►

◄ | ►

Back | Close

Full Screen / Esc

Print Version

Interactive Discussion

like a backward facing inlet, and by providing almost the full positive ram pressure. A minor technical advantage is that Rosemount probes come with the required certification for civil aircraft.

Ryerson et al. (1999) argued that earlier measurements made with a gold converter mounted inside a Rosemount probe seemed to suffer from wall effects in the probe before the air reached the converter (T. Ryerson, private communication). This finding is in contradiction to the results from the MOZAIC humidity/temperature sensor. The absence of a detectable change in the signal of the temperature sensor when the de-icing heater of the Rosemount probe is switched on and off during flight clearly shows that the air sampled through the side arm of the probe has no measurable contact with the wall of the probe. This conclusion is supported by results from an in-flight comparison with a research instrument operated by ETH-Zürich aboard a Learjet as part of the SPURT project, which has the gold converter mounted outside the fuselage without any inlet line. The good agreement between the two instruments limits potential losses of HNO_3 in the MOZAIC inlet to 15% (Pätz et al., in preparation, 2004 [1]).

The suitability of different inlet materials for measurements of HNO_3 was investigated by (Neuman et al., 1999), who found PFA tubing to provide the best time response when kept at temperatures above 20˚C. Different from our results, these authors found PFA and FEP tubing to exhibit a similar memory for HNO_3, whereas we found repeatedly FEP to provide a faster time response. The reasons for the differing results are not clear.

4.3. Converter

During long series of laboratory tests for this and other gold converters deployed, e.g., at Schauinsland (Flocke et al., 1998; Pätz et al., 2000) and aboard the UK research

---

[1]Pätz, H. W., Volz-Thomas, A., Hegglin, M., Brunner, D., and Schmidt, U.: In-situ comparison of the NOy instruments flown in MOZAIC and SPURT, Atmos. Chem. Phys. Discuss., in preparation, 2004.

NO$_y$ instrument aboard MOZAIC in-service aircraft

A. Volz-Thomas et al.

Title Page

Abstract | Introduction

Conclusions | References

Tables | Figures

◄ | ►

◄ | ►

Back | Close

Full Screen / Esc

Print Version

Interactive Discussion

© EGU 2004

aircraft C-130 (Gerbig et al., 1996), we always found the same behaviour in terms of the temperature dependence of the conversion efficiency for NO_2 and HNO_3, as well as PAN and other organic nitrates. Therefore, only the conversion efficiency for NO_2 is checked in flight. The conversion efficiency for HNO_3 is regularly checked during
5 maintenance (see above).

Our results for HNO_3 (Fig. 9) are somewhat different to those obtained by Fahey et al. (1985), who found the conversion efficiency for HNO_3 to be 5–10% smaller than for NO_2. A possible explanation is the larger ratio of tube length to sample flow rate of our converter, which was designed for flow rates up to 300 ml/min. The longer tubes were
10 chosen because of the long operating cycles of the MOZAIC instrument, without the possibility for cleaning in between flights.

Different from Kliner et al. (1997), we found no significant pressure dependence of the conversion efficiency for NO_2 and HNO_3, likely because of the length of our converter and the relatively homogeneous temperature profile.

15 4.4. Specifications and outlook

The features of the MOZAIC NOy-instrument are summarised in Table 1. The sensitivity of 0.4–0.7 cps/ppt with the zero mode signal of about 200 cps gives a statistical detection limit of better than ±30–50 ppt for an integration time of 4 s, i.e. the data storage rate for the MOZAIC data base, and ±150–300 ppt at the maximum resolution of
20 the instrument (10 Hz). The inaccuracy arising from uncertainties in the sensitivity of the CLD and the conversion efficiency during a flight period are ±5% each. A relatively large source of inaccuracy comes from the instrumental background, which in flight is usually 100–200 ppt with an uncertainty of 30–60 ppt. Hence, the overall statistical error of a 4 s NOy measurement (in ppt) is

25 $\Delta NOy = \pm(A * \mu(NOy) + B)$
with $A = 0.07$ and 60 ppt $<B<80$ ppt.

The contributions are added arithmetically to provide a conservative estimate of the overall error, because the absence of correlation between the two terms is not easily argued.

Additional errors arise from interferences and, in case of sharp transients, from the memory for HNO_3. Atmospheric mixing ratios of HCN in the range of 100–300 ppt were reported for springtime over the Pacific during TRACE-P (Singh et al., 2003), with somewhat higher concentrations found in biomass burning plumes. The in-situ measurements were in good agreement with the tropospheric column of HCN (4×10^{15} cm^{-2}) measured over Japan (Zhao et al., 2000). HCN-columns of 2–3×10^{15} cm^{-2} obtained over Jungfraujoch and Mauna Loa (Rinsland et al., 1999; Rinsland et al., 2000), would lead to similar tropospheric mixing ratios, because of the higher altitude of the observatories. Therefore, a significant fraction of the NOy mixing ratios observed in the troposphere with the MOZAIC NOy instrument could in fact be due to HCN. In the lower stratosphere on the other hand, the fraction of HCN is generally below 10% because of the higher concentrations of HNO_3 (Neuman et al., 1999) and the slightly lower values of HCN.

The NOy instrument has been flown continuously aboard a MOZAIC A-340 aircraft operated by Deutsche Lufthansa on more than 1800 flights (>10 000 h with data) since April 2001. About 40% of the data recovered had a lower accuracy than described above, because of deterioration of the sensitivity or conversion efficiency or because of increased memory, usually due to contamination occurring during an operation cycle. Such data were not submitted to the MOZAIC data base. An example for the performance during flight is given in Fig. 11. Both NOy and O_3 mixing ratios increase whenever the aircraft enters the stratosphere. In the troposphere, NOy shows a much larger variance than O_3. The right panel shows the scatter plot between O_3 and NOy. The slope of 200 (mole O_3 per mole NO_y) found in the stratospheric data, corresponds to a NOy/O_3 ratio of 5 ppt/ppb, which is slightly higher than the results obtained during flights with the NASA ER-2 aircraft (Fahey et al., 1996; Murphy et al., 1993).

An in-flight comparison with a research instrument operated by ETH-Zürich was con-

ducted in April 2003. As will be discussed in detail in Pätz et al. (in preparation, 2004)[1], the two instruments agreed within their specified uncertainties. The systematically lower measurements of the MOZAIC instrument may, however, indicate the presence of small (<15%) losses of HNO_3 in the MOZAIC inlet system.

References

Brunner, D., Staehelin, J., Jeker, D., Wernli, H., and Schumann, U.: Nitrogen oxides and ozone in the tropopause region of the Northern Hemisphere: Measurements from commercial aircraft in 1995/96 and 1997, J. Geophys. Res., 106, 27 673–27 699, 2001.

Chameides, W. and Walker, J. C. G.: A Photochemical Theory of Tropospheric Ozone, J. Geophys. Res., 78, 8751–8760, 1973.

Clough, P. N. and Thrush, B. A.: Mechanism of the Chemiluminescent Reaction Between NO and O3, Transactions of the Faraday Society, 63, 915–925, 1967.

Crutzen, P. J.: A discussion of the chemistry of some minor constituents in the stratosphere and troposphere, Pure Appl. Geophys., 106–108, 1385–1399, 1973.

Drummond, J. W., Volz, A., and Ehhalt, D. H.: An optimized chemiluminescence detector for tropospheric NO measurements, J. Atmos. Chem., 2, 287–306, 1985.

Emmons, L. K., Carroll, M. A., Hauglustaine, D. A., Brasseur G. P., Atherton, C., Penner, J., Sillman, S., Levy II, H., Rohrer, F., Wauben, W. M. F., Velthoven, P. F. J. V., Wang, Y., Jacob, D., Bakwin, P., Dickerson, R., Doddridge, B., Gerbig, C., Honrath, R., Hübler, G., Jaffe, D., Kondo, Y., Munger, J. W., Torres, A., and Volz-Thomas, A.: Climatologies of NOx and NOy: a comparison of data and models, Atm. Env., 31, 1851–1904, 1997.

NO$_y$ instrument aboard MOZAIC in-service aircraft

A. Volz-Thomas et al.

Title Page

Abstract	Introduction
Conclusions	References
Tables	Figures

|◄ | ►|
| ◄ | ► |

Back | Close

Full Screen / Esc

Print Version

Interactive Discussion

© EGU 2004

Title Page

Abstract	Introduction
Conclusions	References
Tables	Figures

◄◄   ►►

◄   ►

Back   Close

Full Screen / Esc

Print Version

Interactive Discussion

© EGU 2004

Emmons, L. K., Hauglustaine, D. A., Muller, J.-F., Caroll, M. A., Brasseur, G. P., Brunner, D., Staehelin, J., Thouret, V., and Marenco, A.: Data composites of airborne observations of tropospheric ozone and its precursors, J. Geophys. Res., 105, 20 497–20 538, 2000.

Fahey, D. W., Eubank, C. S., H'ubler, G., and Fehsenfeld, F. C.: Evaluation of a Catalytic Reduc-
5   tion Technique for the Measurement of Total Reactive Odd-Nitrogen NOy in the Atmosphere. J. Atmos. Chem., 3, 435–468, 1985.

Fahey, D. W., Donnelly, S. G., Keim, E. R., Gao, R. S., Wamsley, R. C., Delnegro, L. A., Wood-
bridge, E. L., Proffitt, M. H., Rosenlof, K. H., Ko, M. K. W., Weisenstein, D. K., Scott, C. J., Nevison, C., Solomon, S., and Chan, K. R.: In situ observations of NOy, O3, and the NOy/O3
10   ratio in the lower stratosphere. Geophys. Res. Lett., 23, 1653–1656, 1996.

Fahey, D. W., Gao, R. S., Carslaw, K. S., Kettleborough, J., Popp, P. J., Northway, M. J., Holecek, J. C., Ciciora, S. C., McLaughlin, R. J., Thompson, T. L., Winkler, R. H., Baumgardner, D. G., Gandrud, B., Wennberg, P. O., Dhaniyala, S., McKinney, K., Peter, T., Salawitch, R. J., Bui, T. P., Elkins, J. W., Webster, C. R., Atlas, E. L., Jost, H., Wilson, J. C., Herman, R. L., Kleinböhl,
15   A., and v. König, M.: The Detection of Large HNO3-Containing Particles in the Winter Arctic Stratosphere, Science, 291, 1026–1031, 2001.

Flocke, F., Volz-Thomas, A., Buers, H.-J., Pätz, W., Garthe, H.-J., and Kley, D.: Long-term Measurements of Alkyl Nitrates in Southern Germany, 1. General Behaviour, Seasonal and Diurnal Variation, J. Geophys. Res., 103, 5729–5746, 1998.

20   Gerbig, C., Kley, D., Volz-Thomas, A., Kent, J., Dewey, K., and McKenna, D. S.: Fast-Response Resonance Fluorescence CO Measurements Aboard the C-130: Instrument Characteriza-
tion and Measurements Made During NARE '93, J. Geophys. Res., 101, 29 229–29 238, 1996.

Gierens, K., Schumann, U., Helten, M., Smit, H. G. J., and Marenco, A.: A distribution law for
25   relative humidity in the upper troposphere and lower stratosphere derived from three years of MOZAIC measurements, Ann. Geophys., 17, 1218–1226, 1999,
SRef-ID: 1432-0576/ag/1999-17-1218.

Helten, M., Smit, H. G. J., Straeter, W., Kley, D., Nedelec, P., Zöger, M., and Busen, R.: Calibra-
tion and Performance of Automatic Compact Intrumentation for the Measurement of Relative
30   Humidity from Passenger Aircraft, J. Geophys. Res., 103, 25 643–25 652, 1998.

Helten, M., Smit, H. G. J., Kley, D., Ovarlez, J., Schlager, H., Baumann, R., Schumann, U., Nedelec, P., and Marenco, A.: In-flight intercomparison of MOZAIC and POLINAT water vapor measurements, J. Geophys. Res., 104, 26 087–26 096, 1999.

Kliner, D. A. V., Daube, B. C., Burley, J. D., and Wofsy, S. C.: Laboratory investigation of the catalytic reduction technique for measurement of atmospheric NOy, J. Geophys. Res., 102, 10 759–10 776, 1997.

Liu, S. C., Kley, D., McFarland, M., Mahlman, J. D., and Levy, H.: On the origin of tropospheric ozone, J. Geophys. Res., 85, 7546–7552, 1980.

Marenco, A., Thouret, V., Nedelec, P., Smit, H., Helten, M., Kley, D., Karcher, F., Simon, P., Law, K., Pyle, J., Poschmann, G., von Wrede, R., Hume, C., and Cook, T.: Measurement of ozone and water vapor by Airbus in-service aircraft: The MOZAIC airborne program, An overview, Geophys. Res.-Atmos., 103, 25 631–25 642, 1998.

Murphy, D. M., Fahey, D. H., Proffitt, M. H., Liu, S. C., Chan, K. R., Eubank, C. S., Kawa, S. R., and Kelly, K. K.: Reactive Nitrogen and its Correlation With Ozone in the Lower Stratosphere and Upper Troposhere, J. Geophys. Res., 98, 8751–8773, 1993.

Murphy, D. M. and Fahey, D. W.: An Estimate of the Flux of Stratospheric Reactive Nitrogen and Ozone into the Troposphere, J. Geophys. Res., 99, 5325–5332, 1994.

Neuman, J. A., Huey, L. G., Ryerson, T. B., and Fahey, D. W.: Study of Inlet Materials for Sampling Atmospheric Nitric Acid, Environmental Science & Technology, 33, 1133–1136, 1999.

Neuman, J. A., Gao, R. S., Fahey, D. W., Holecek, J. C., Ridley, B. A., Walega, J. G., Grahek, F. E., Richard, E. C., McElroy, C. T., Thompson, T. L., Elkins, J. W., Moore, F. L., and Ray, E. A.: In situ measurements of HNO3, NOy, NO, and O3 in the lower stratosphere and upper troposphere, Atm. Env., 35, 5789–5797, 2001.

Pätz, H.-W., Corsmeier, U., Glaser, K., Kalthoff, N., Kolahgar, B., Klemp, D., Lerner, A., Neininger, B., Schmitz, T., Schultz, M., Slemr, J., Vogt, U., and Volz-Thomas, A.: Measurements of trace gases and photolysis frequencies during SLOPE96 and a coarse estimate of the local OH concentration from HNO3 formation, J. Geophys. Res., 105, 1563–1583, 2000.

Richter, A. and Burrows, J. P.: Retrieval of tropospheric NO2 from GOME measurements, Adv. Space Res., 29, 1673–1683, 2002.

Ridley, B. A. and Grahek, F. E.: A small, low flow, high sensitivity reaction vessel for NO/O3 chemiluminescence detectors, Journal Atmospheric Oceanic Technology, 7, 307–311, 1990.

Rinsland, C. P., Goldman, A., Murcray, F. J., Stephen, T. M., Pougatchev, N. S., Fishman, J., David, S. J., Blatherwick, R. D., Novelli, P. C., Jones, N. B., and Connor, B. J. : Infrared solar spectroscopic measurements of free tropospheric CO, C2H6, and HCN above Mauna Loa,

Hawaii: Seasonal variations and evidence for enhanced emissions from the Southeast Asian tropical fires of 1997–1998. J. Geophys. Res., 104, 18 667–18 680, 1999.

Rinsland, C. P., Mahieu, E., Zander, R., Demoulin, P., Forrer, J., and Buchmann, B.: Free tropospheric CO, C2H6, and HCN above central Europe: Recent measurements from the Jungfraujoch station including the detection of elevated columns during 1998, J. Geophys. Res., 105, 24 235–24 249, 2000.

Ryerson, T. B., Huey, L. G., Knapp, K., Neuman, J. A., Parrish, D. D., Sueper, D. T., and Fehsenfeld, F. C.: Design and initial characterization of an inlet for gas-phase NOy measurements from aircraft, J. Geophys. Res., 104, 5483, 1999.

Singh, H. B., Salas, L., Herlth, D., Kolyer, R., Czech, E., Viezee, W., Li, Q., Jacob, D. J., Blake, D., Sachse, G., Harward, C. N., Fuelberg, H., Kiley, C. M., Zhao, Y., and Kondo, Y.: In situ measurements of HCN and CH3CN over the Pacific Ocean: Sources, sinks, and budgets, J. Geophys. Res., 108, 8795, 2003.

Thouret, V., Marenco, A., Nedelec, P., and Grouhel, C.: Ozone climatologies at 9–12 altitude as seen by the MOZAIC airborne program between September 1994 and August 1996, J. Geophys. Res., 103, 25 653–25 679, 1998.

Thouret, V., Cho, J. Y. N., Newell, R. E., Marenco, A., and Smit, H. G. J.: General characteristics of troposphereic trace constituent layers observed inthe MOZAIC program, J. Geophys. Res., 105, 17 379–17 392, 2000.

Weinheimer, A. J., Campos, T. L., and Ridley, B. A.: The in-flight sensitivity of gold-tube NOy converters to HCN, Geophys. Res. Lett., 25, 3943–3946, 1998.

Zhao, Y., Kondo, Y., Murcray, F. J., Liu, X., Koike, M., Irie, H., Strong, K., Suzuki, K., Sera, M., and Ikegami, M.: Seasonal variations of HCN over northern Japan measured by ground-based infrared solar spectroscopy, Geophys. Res. Lett., 27, 2085–2088, 2000.

NO$_y$ instrument aboard MOZAIC in-service aircraft

A. Volz-Thomas et al.

Title Page

Abstract	Introduction
Conclusions	References
Tables	Figures

⏮ ⏭

◀ ▶

Back Close

Full Screen / Esc

Print Version

Interactive Discussion

NO$_y$ instrument aboard MOZAIC in-service aircraft

A. Volz-Thomas et al.

**Table 1.** Specifications of the MOZAIC NOy-instrument.

Specification	Quantity	Remarks
Size (w, l, h)	$30 \times 70 \times 30\,\mathrm{cm}^3$	including calibration system and pump
Weight	$50\,\mathrm{kg}$	including fixation and 20L O2 cylinder
Sensitivity	$0.5\,\mathrm{cps/ppb}$	0.3–0.7, depending on PMT etc.
data acquisition rate	$10\,\mathrm{Hz}$	PMT signal
	$1\,\mathrm{Hz}$	housekeeping data
time resolution	0.1 s (NOx)	
	20 s (HNO3)	due to memory in the inlet line
Endurance	>5 weeks	assuming full operation of aircraft
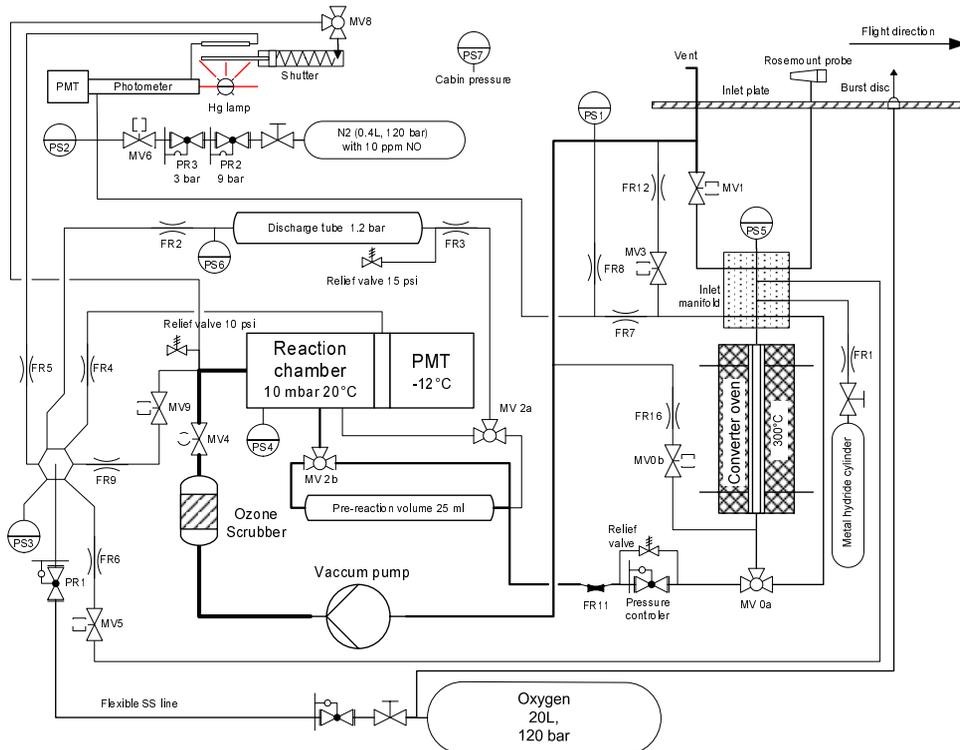
Fig. 1. Schematics of the MOZAIC NOy-instrument (FRn: flow restrictors, i.e., capillaries or critical orifices; PSn: pressure sensors; PR: pressure regulators; MVn: magnetic valves).
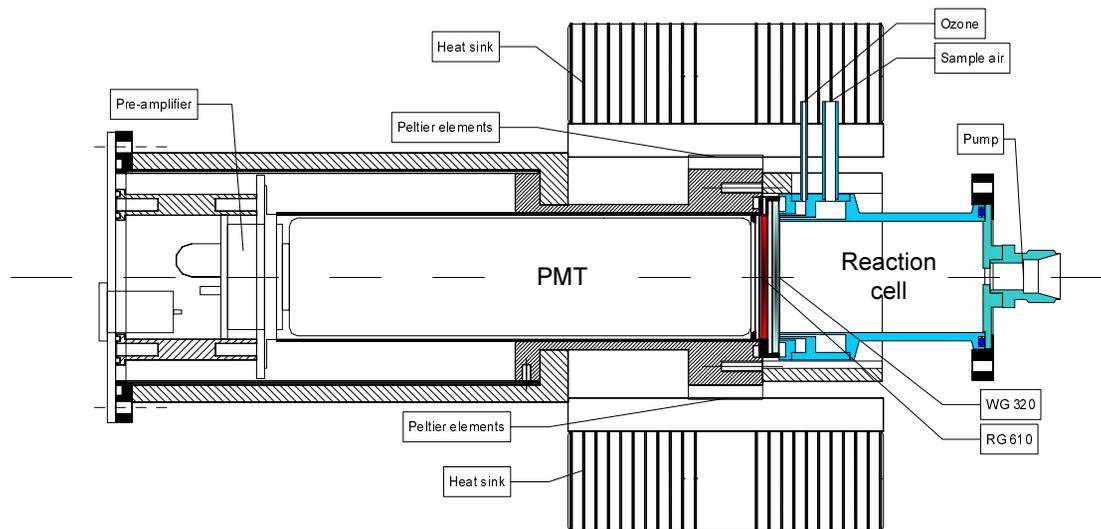
Fig. 2. Details of the CLD.

Title Page

Abstract | Introduction

Conclusions | References

Tables | Figures

◄◄ | ►►

◄ | ►

Back | Close

Full Screen / Esc

Print Version

Interactive Discussion
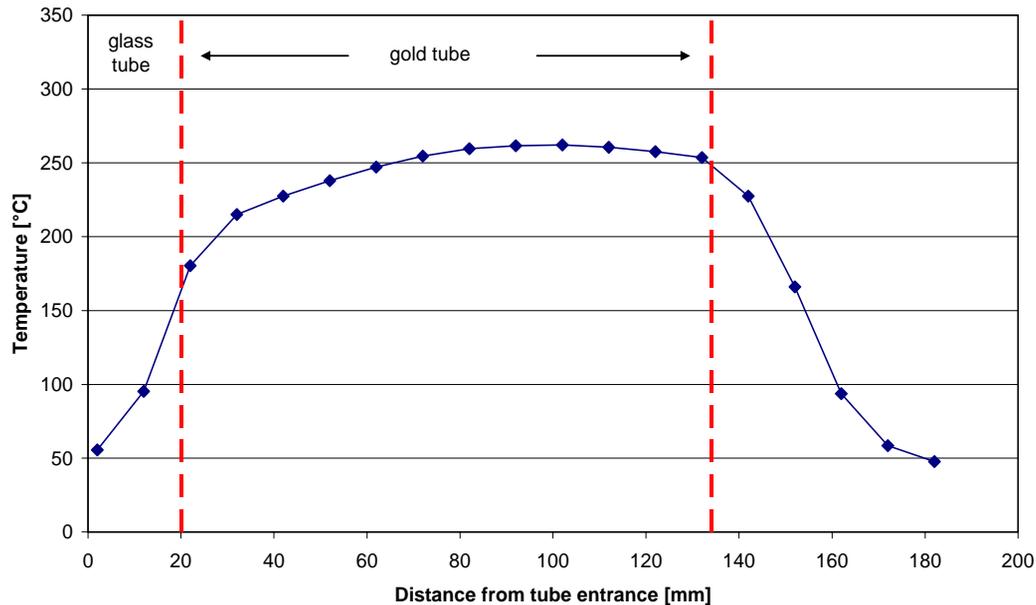
Fig. 3. Temperature profile measured inside the tube for a setting of the temperature controller of 300C.
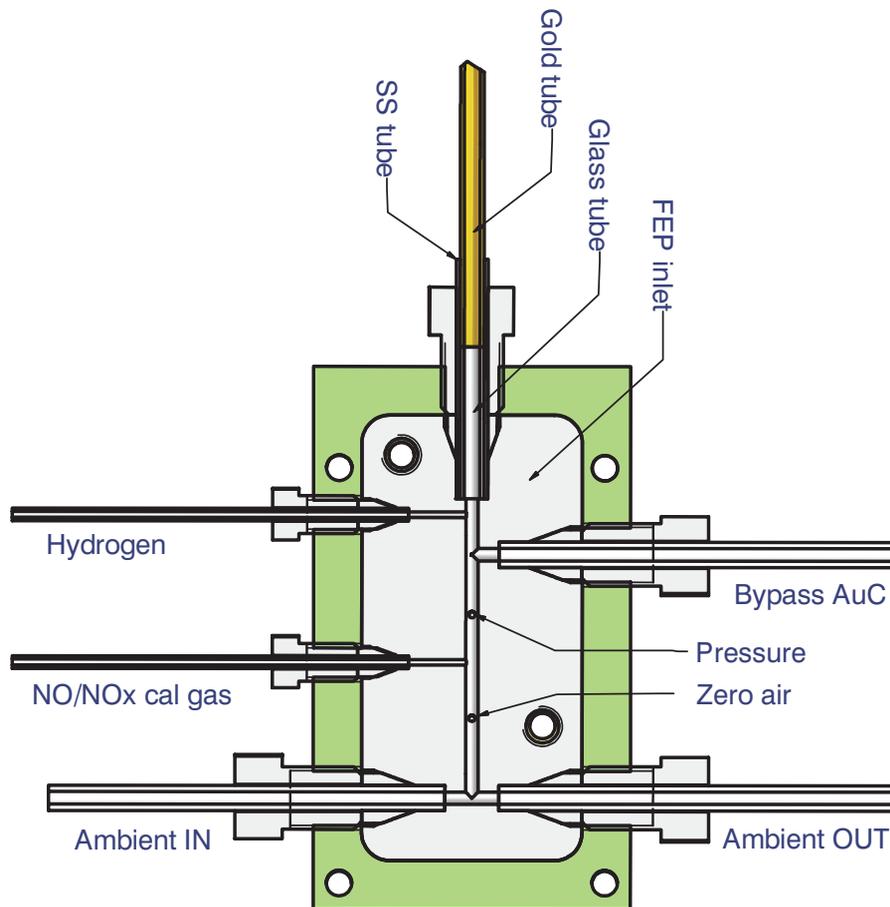
Fig. 4. Details of the inlet manifold and connection of the catalytic converter.
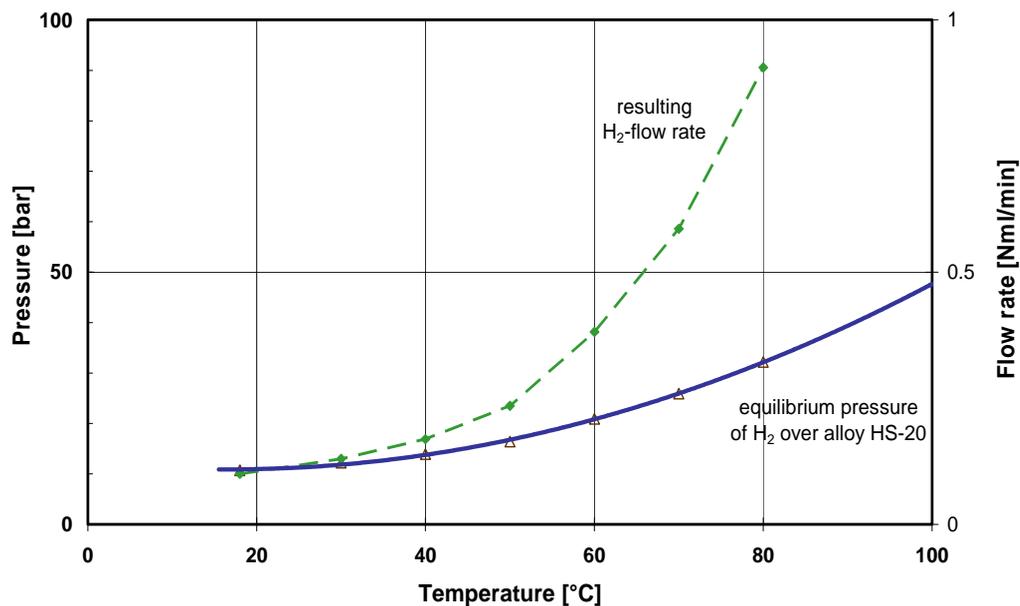
Fig. 5. Temperature dependence of the H$_2$ pressure over the Ti-alloy (triangles) and the corresponding H$_2$ flow rate (diamonds).
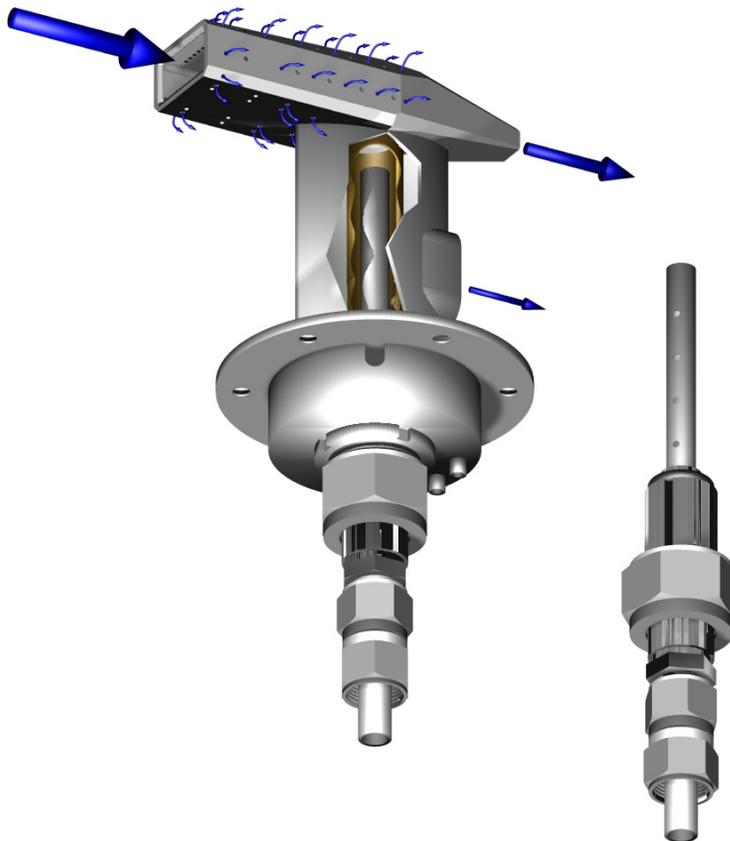
Fig. 6. Drawing of the Rosemount probe and the NOy inlet line. The arrows indicate the air flow.

Title Page

Abstract | Introduction

Conclusions | References

Tables | Figures

◄ | ►

◄ | ►

Back | Close

Full Screen / Esc

Print Version

Interactive Discussion

© EGU 2004
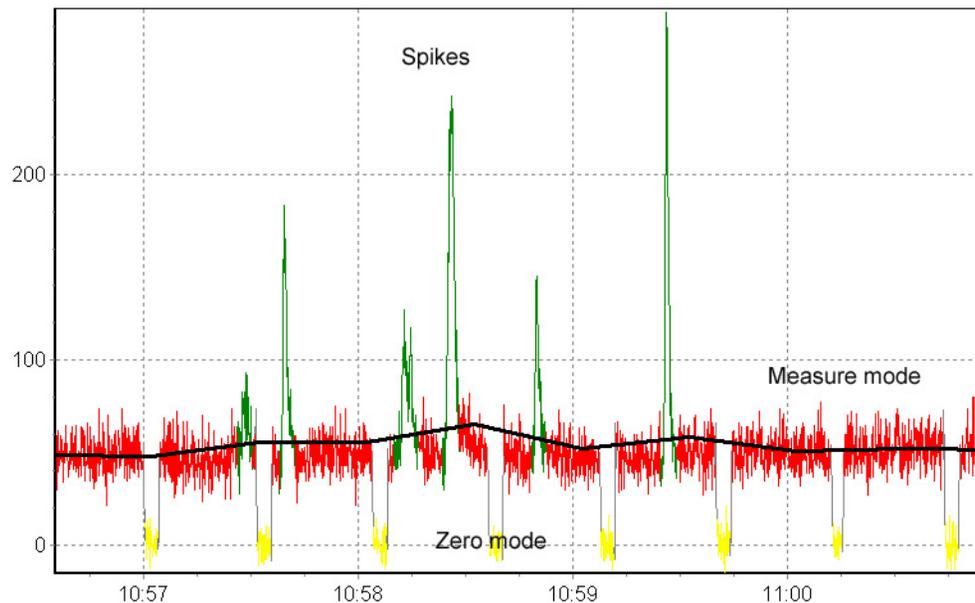
Fig. 7. Example of the raw data sampled at 10 Hz during in-flight operation with several spikes of recent plumes.
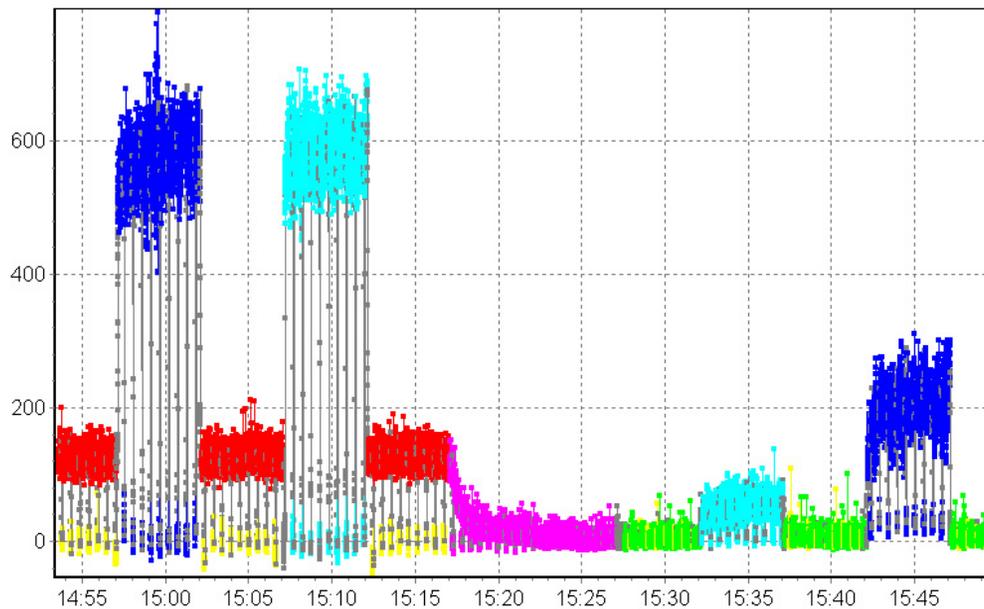
Fig. 8. Example for an in-flight calibration cycle (red/green: CLD measure modes ambient air for NO$_y$ and NO; yellow: CLD zero mode; blue: NO calibration added to ambient in NO$_y$ and NO modes; turquois: NO$_2$ calibration in NO$_y$ and NO modes; pink: zero air in NO$_y$ and NO modes).
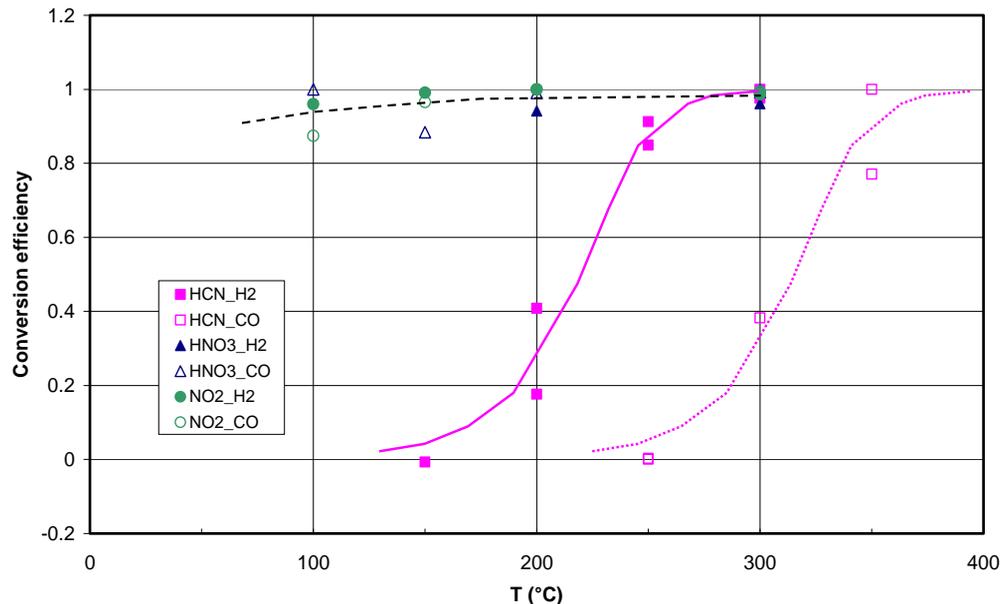
Fig. 9. Conversion efficiency of the gold converter for NO$_2$ (circles, 7.7 ppb), HNO$_3$ (triangles, 9.7 ppb), and HCN (squares, 71 ppb), as a function of temperature at a pressure of 250 mb. Open and filled symbols refer to experiments with CO and H$_2$, respectively (flow rate 0.2 ml/min). Results for NH$_3$ are not shown, as the conversion efficiency was always <1% at temperatures up to 400˚C. The temperature scale at the abscissa corresponds to the setting of the controller. The actual temperature of the gold tube is somewhat lower (see Fig. 3).
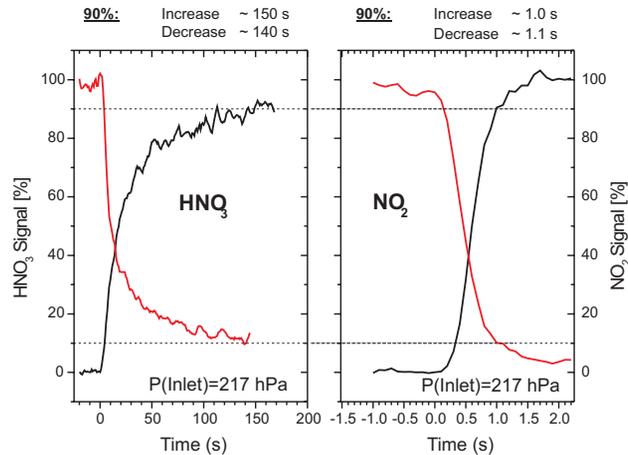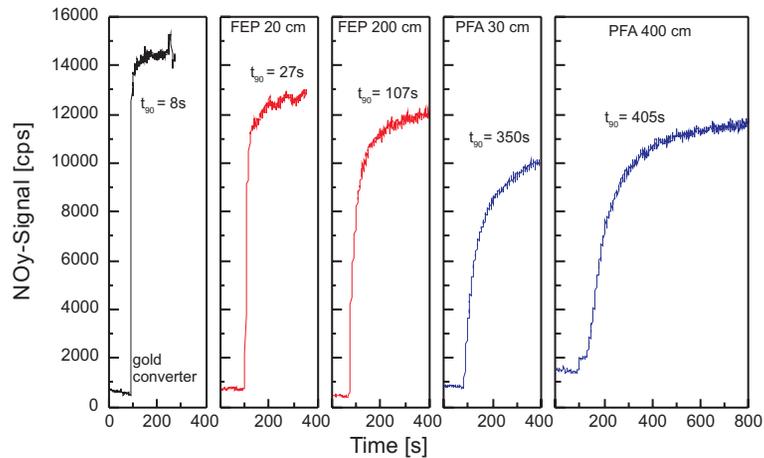
Fig. 10. Time response of the gold tube and different inlet line materials (upper panel) and time response of the actual MOZAIC inlet line (80 cm FEP) for NO_2 and HNO_3 (lower panel).
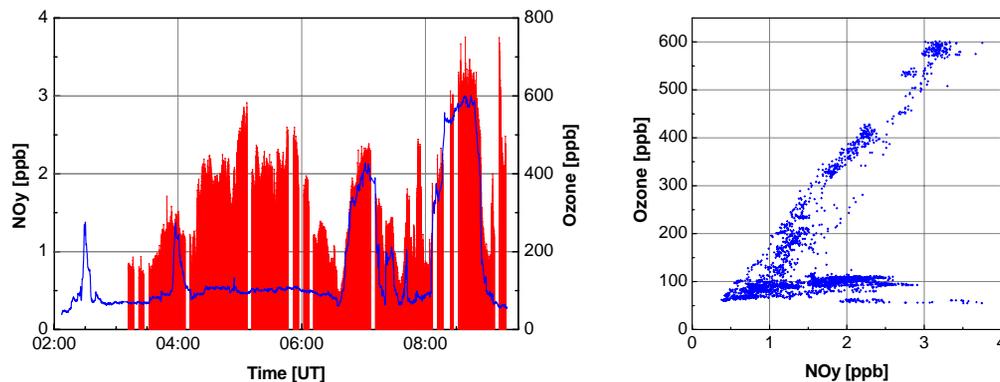
Fig. 11. Left: Time series of NO$_y$ (red bars) and O3 (blue line) from a MOZAIC flight from Boston to Frankfurt in May 2001. The data gaps are due to calibration and background determinations. Right: Scatter plot of O$_3$ vs. NO$_y$.